Takahashi, S., & Nagayama, K. (1988) *J. Magn. Reson. 76*, 347-351.
Wüthrich, K. (1986) in *NMR of Proteins and Nucleic Acids* John Wiley, New York.
Wüthrich, K., Billeter, M., & Braun, W. (1983) *J. Mol. Biol. 169*, 949-961.
Zuiderweg, E. P. R., Hallenga, K., & Olejniczak, E. T. (1986) *J. Magn. Reson. 70*, 336-343.

Photoinduced Destabilization of Liposomes†

Henry Lamparski, Ulrich Liman, Judith A. Barry, David A. Frankel, V. Ramaswami, Michael F. Brown, and David F. O'Brien*

C. S. Marvel Laboratories, Department of Chemistry, University of Arizona, Tucson, Arizona 85721

Received July 15, 1991; Revised Manuscript Received October 11, 1991

ABSTRACT: The stability of two-component liposomes composed of the polymerizable 1,2-bis-[10-(2',4'-hexadienoyloxy)decanoyl]-*sn*-glycero-3-phosphatidylcholine (SorbPC) and either a phosphatidylethanolamine (PE) or a phosphatidylcholine (PC) were examined via fluorescence leakage assays. Ultraviolet light exposure of SorbPC-containing liposomes forms poly-SorbPC, which phase separates from the remaining monomeric lipids. If the nonpolymerizable lipids are PE's, then the photoinduced polymerization destabilizes the liposome with loss of aqueous contents. The permeability of the control dioleoylPC/SorbPC membranes was not affected by photopolymerization of SorbPC. The photodestabilization of dioleoylPE/SorbPC (3:1) liposomes required the presence of oligolamellar liposomes. NMR spectroscopy of extended bilayers of dioleoylPE/SorbPC (3:1) showed that the photopolymerization lowers the temperature for the appearance of ^{31}P NMR signals due to the formation of isotropically symmetric lipid structures. These observations suggest the following model for the photoinduced destabilization of liposomes composed of PE/SorbPC: photopolymerization induced phase separation with the formation of enriched domains of PE, which allows the close approach of apposed regions of enriched PE lamellae and permits the formation of an isotropically symmetric structure between the lamellae. The formation of such an interlamellar attachment (ILA) between the lamellae of an oligolamellar liposome provides a permeability pathway for the light-stimulated leakage of entrapped water-soluble reagents.

Several classes of biological lipids form hydrated membrane systems that display a variety of lamellar and nonlamellar phases as a function of temperature, pressure, and concentration. The formation of nonlamellar structures in membranes has been extensively investigated in recent years due to interest in their possible cell membrane role in the processes of fusion, endo- and exocytosis, and the transmembrane movement of large molecules [reviewed by Verkleij (1984), Cullis et al. (1985), Gruner et al. (1987), Hui (1988), Lindblom and Rilfors (1989), and Seddon (1990)].

Membranes composed of PE's, e.g., DOPE, are capable of forming inverted hexagonal (H_{II})[1] or inverted cubic (Q_{II}) phases. The H_{II} phase was first observed in the X-ray diffraction studies of Luzzati and co-workers in the 1960s (Luzzati & Reiss-Husson, 1962; Luzzati et al., 1968). It can also be detected by ^{31}P NMR (Cullis & de Kruijff, 1979) and ^{2}H NMR (Tilcock et al., 1982), by enhancement of the fluorescence intensity of lipid probes (Ellens et al., 1986a; Bentz et al., 1987; Hong et al., 1988), by differential scanning calorimetry (Van Dijck et al., 1976; Cullis & de Kruijff, 1978; Epand, 1985; Ellens et al., 1986a,b), and visualized by freeze-fracture electron microscopy (Deamer et al., 1970; Gulik-Krzywicki, 1975; Hui et al., 1981) as well as cryomicroscopy (Siegel et al., 1989a; Talmon et al., 1990).

Frequently a phase with isotropic symmetry (Luzzati & Reiss-Husson, 1962) is found between the lamellar and the hexagonal phases (Lindblom & Rilfors, 1989). In some instances it is observed only after the hydrated lipid sample is cycled several times through the temperature region of T_H (Shyamsunder et al., 1988; Veiro et al., 1990). Phospholipid membranes that show this metastable Q_{II} phase exhibit cubic X-ray diffraction patterns, isotropic ^{31}P NMR spectra (Cullis & de Kruijff, 1979; Hui et al., 1983), and lipidic particles in freeze-fracture electron microscopy images (Hui et al., 1981, 1983; Tilcock et al., 1982; Verkleij et al., 1982; Epand & Bottega, 1988). Ellens et al. (1986b) presented evidence that lipid membranes that exhibit isotropic structures are able to fuse with neighboring liposomes. Bentz et al. (1987) assert that lipid membranes that begin, but do not rapidly complete, the transition from lamellar to the hexagonal phase are likely to be fusion competent [see also Ellens et al. (1989) and Siegel et al. (1989b)].

PE liposomes are generally unstable at physiological pH unless they also consist of other lipids such as PC (Stollery & Vail, 1977). Processes which lead to the phase separation of PE and other lipids can trigger the lamellar to nonlamellar phase transition(s) (Ellens et al., 1984, 1986b; Conner et al.,

† This research was supported in part by a National Science Foundation Grant DMR-8722341 (D.F.O.), by a National Institutes Health Grant GM41413 (M.F.B.), by funds provided by the University of Arizona, and by a Deutsche Forschungsgemeinschaft fellowship (U.L.) and a National Institutes of Health postdoctoral fellowship (J.A.B.).

[1] Abbreviations: ANTS, 8-Aminonaphthalene-1,3,6-trisulfonic acid disodium salt; CHEMS, cholesteryl hemisuccinate; DMF, dimethylforamide; DOPC, dioleoylphosphatidylcholine; DOPE, dioleoylphosphatidylethanolamine; DOPE-Me, *N*-methylated dioleoylphosphatidylethanolamine; DPX, *p*-xylylenebispyridinium bromide; GPC, L-α-glycerophosphorylcholine; T_H, lamellar liquid-crystalline/hexagonal phase transition; H_{II}, inverted hexagonal phase; NMR, nuclear magnetic resonance; PE, phosphatidylethanolamine; Q_{II}, inverted cubic phase; SorbPC, 1,2-bis-[10-(2',4'-hexadienoyloxy)decanoyl]-*sn*-glycero-3-phosphatidylcholine; THF, tetrahydrofuran; TES, *N*-[Tris(hydroxymethyl)-methyl]-2-aminoethanesulfonic acid; TPE, PE prepared from egg phosphatidylcholine by transphosphatidylation.

0006-2960/92/0431-685$03.00/0

1984; Duzgunes et al., 1985; Leventis et al., 1986; Brown & Silvius, 1989). Thus the lateral distribution of lipids can modify the local phase behavior of PE. Research on PE polymorphorism has lead to the development of several methods to modulate the local phase behavior of membranes and cause their destabilization by the addition of ions, protons, antibiotics, and peptides.

In this paper, we describe the *light*-induced destabilization and aqueous contents leakage of liposomes composed of PE's and a photopolymerizable lipid bis-SorbPC (**1**). The light-

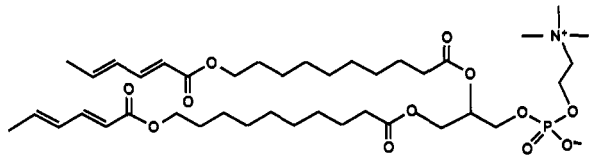

bis-SorbPC (1)

mediated release of water-soluble reagents from liposomes has previously been accomplished via the trans–cis photoisomerization of azobenzene substituted lipids (Kano et al., 1981) or retinyl substituted lipids (Pidgeon & Hunt, 1983, 1987), the photolytic modification of the lipid head group (Haubs & Ringsdorf, 1985, 1987), as well as the photogeneration of acid in the presence of pH-sensitive liposomes (You & Tirrell, 1991).

The method described here utilizes the photopolymerization of lipid bilayers. Although the polymerization of bilayers is generally associated with the chemical and physical stabilization of liposomes [reviewed by O'Brien and Ramaswami (1989), Ringsdorf et al. (1988), Regen (1987), and Bader et al. (1985)], the polymerization of reactive lipids in two- or multicomponent membranes can cause the phase separation of the polymerized lipid from the colipid(s) (Gaub et al., 1984; Tyminski et al., 1985, 1988). If the colipid prefers a lamellar structure, the newly formed phase-separated liposome will retain both its size and encapsulation characteristics. Recently, we have discovered that the opposite effect is obtained if the colipid is polymorphic [see preliminary reports by Liman et al. (1988) and Frankel et al. (1989)]. The ability to trigger the formation of nonlamellar phases significantly increases the permeability of liposomes to water-soluble markers. This new method for the destabilization of liposomes opens the possibility of photocontrol of the release of reagents in a spatially and temporally selective manner.

Materials and Methods

Materials

DOPE, DOPC, egg PE prepared by transphosphatidylation (TPE), and *N*-(7-nitro-2,1,3-benzoxadiazol-4-yl)-PE (NBD-PE) were obtained from Avanti Polar Lipids and used without purification (one spot TLC, 65:25:4 $CHCl_3/MeOH/H_2O$). L-Glycerophosphorylcholine cadmium chloride (GPC-$CdCl_2$) was purchased from Sigma Chemical Co. 8-Aminonaphthalene-1,3,6-trisulfonic acid disodium salt (ANTS) and *p*-xylylenebispyridinium bromide (DPX) were supplied by Molecular Probes, Inc. *N*-[Tris(hydroxymethyl)methyl]-2-aminoethanesulfonic acid (TES) and calcein (Sigma) were used as received. Octylphenoxypoly(ethoxyethanol) (Triton X-100) (Sigma) was diluted with Millipore water (5% w/w). All buffers were prepared with Milli-Q water.

10-(2',4'-Hexadienoyloxy)decan-1-ol. 2,4-Hexadienoic acid (71.6 g, 0.64 mol) was converted to the corresponding acid chloride by the dropwise addition of oxalyl chloride (100 g, 0.79 mol) and stirred at room temperature overnight. The resulting yellow solution was concentrated and vacuum distilled at 50 °C (760 mm Hg) to give a yield in excess of 90%. The freshly distilled sorbyl chloride (31.0 g, 0.24 mol) was taken up in THF (100 mL) and added dropwise over 2 h to a mixture of 1,10-decanediol (151.6 g, 0.87 mol) and pyridine (80 g, 1.01 mol) in THF (1.5 L) followed by stirring overnight. The pyridine-HCl salt was filtered off, and the yellow filtrate was concentrated by rotary evaporation. Upon addition of CCl_4 (400 mL) and cooling to −10 °C for 3 h, excess 1,10-decanediol precipitated and was filtered off. The filtrate was evaporated to an oil, and the crude product was extracted by boiling in hexane (4 × 300 mL) and decanting off from the sludge remaining on the bottom of the flask. Once cooled, Celite (50 g) was added to the extracted hexane, boiled for several minutes, and filtered hot. Precipitation of the desired compound occurred after it was cooled to 4 °C and allowed to stand for two days. The product was further purified by flash silica gel chromatography (eluent CH_2Cl_2). Yield 36.7 g (56%); mp 33–34 °C. TLC R_f = 0.80–0.75 ($CHCl_3/CH_3OH$, 99:1). ^1H NMR ($CDCl_3$): d 1.20–1.40 (br s, 12 H, $C\underline{H}_2$), 1.45–1.65 (m, 4 H, $C\underline{H}_2CH_2R$), 1.70 (s, 1 H, OH), 1.76–1.85 (d, 3 H, $C{=}CHC\underline{H}_3$), 3.52–3.65 (t, 2 H, $C\underline{H}_2OH$), 4.04–4.13 (t, 2 H, $CO_2C\underline{H}_2$), 5.68–5.79 (d, 1 H, $C{=}C\underline{H}CO_2$), 6.05–6.22 (m, 2 H, $CH_3C\underline{H}{=}C\underline{H}$-), 7.12–7.27 (m, 1 H, $C\underline{H}{=}CHCO_2$). UV: λ_{max} = 258 nm, CH_3OH, ϵ = 25 500.

10-(2',4'-Hexadienoyloxy)decanoic Acid. 10-(2',4'-Hexadienoyloxy)decan-1-ol (20.1 g, 0.075 mol) in DMF (75 mL) was added dropwise to pyridinium dichromate (80.4 g, 0.21 mol) in DMF (75 mL) over 2 h at 4 °C. The reaction mixture was warmed up slowly to room temperature and stirred for 24 h. The dark red suspension was poured into water (500 mL) and extracted with diethyl ether (6 × 150 mL). The organic solutions were combined and washed with 5% HCl (3 × 150 mL) and saturated sodium chloride (3 × 150 mL) and dried over anhydrous sodium sulfate. The filtrate was reduced to a small bulk upon which silica gel (100 g, Aldrich) was added and the slurry left to stand for 1 h with periodic stirring. The silica gel was filtered off and the crude product extracted by boiling in petroleum ether (2 × 500 mL). Fatty acid precipitated after the filtrate was allowed to stand in the freezer (−10 °C) for 3 days. The product was further purified by flash silica gel chromatography (eluent CH_2Cl_2/CH_3OH, 98:2). Yield 11.1 g (52%); mp 54–55 °C. TLC: R_f = 0.25–0.1 ($CHCl_3/CH_3OH$, 95:5). ^1H NMR ($CDCl_3$): d 1.20–1.40 (br s, 10 H, $C\underline{H}_2$), 1.52–1.70 (m, 4 H, $C\underline{H}_2CH_2R$), 1.78–1.86 (d, 3 H, $C{=}CHC\underline{H}_3$), 2.28–2.37 (t, 2 H, $C\underline{H}_2CO_2H$), 4.05–4.15 (t, 2 H, $CO_2C\underline{H}_2$), 5.70–5.79 (d, 1 H, $C{=}C\underline{H}CO_2$), 6.05–6.22 (m, 2 H, $CH_3C\underline{H}{=}C\underline{H}$-), 7.15–7.27 (m, 1 H, $C\underline{H}{=}CHCO_2$). UV: λ_{max} = 258 nm, CH_3OH, ϵ = 25 100.

1,2-Bis[10-(2',4'-hexadienoyloxy)decanoyl]-sn-glycero-3-phosphatidylcholine (bis-SorbPC). L-Glycerophosphorylcholine–cadmium chloride complex (460 mg, 1.04 mmol) was dried by repeated (4×) evaporation from a benzene suspension (5 mL), followed by drying at high vacuum overnight. The residue was mixed with polymerizable fatty acid (1.10 g, 3.90 mmol) and 4-(dimethylamino)pyridine (265 mg, 2.17 mmol) and suspended in 8 mL of chloroform. 1,3-Dicyclohexylcarbodiimide (700 mg, 3.39 mmol) was added, and the mixture was stirred at room temperature for 5 days in the dark under nitrogen. The white suspension was filtered to remove urea, washed with $CHCl_3$ (2 × 15 mL), and concentrated on the rotary evaporator. Methanol (15 mL) was added to the residue and filtered, and the precipitate was washed with methanol (2 × 15 mL). Bio-Rad AG501 ion exchange resin (7 g) was added to the filtrate, and the mixture was stirred for 2 h,

filtered to remove the resin, and washed with $CHCl_3/CH_3OH$, 1:1 (2 × 20 mL). The filtrate was reduced to a small volume and placed on a flash silica gel column (2.5 × 35 cm). Eluting solvents consisted of various mixtures of dichloromethane and methanol: 200 mL of 100% CH_2Cl_2; 250 mL of 90% CH_2Cl_2; 500 mL of 80% CH_2Cl_2; 250 mL of 60% CH_2Cl_2; 500 mL of 50% CH_2Cl_2; 500 mL of 40% CH_2Cl_2; and 750 mL of 20% CH_2Cl_2. The lipid fraction was purified a second time by flash silica gel chromatography (1.0 × 25 cm) using the following solvent gradient: 150 mL of 100% CH_2Cl_2; 150 mL of 90% CH_2Cl_2; 200 mL of 80% CH_2Cl_2; 300 mL of 50% CH_2Cl_2; and 400 mL of 20% CH_2Cl_2. Fractions containing the lipid were rotovaped at room temperature to approximately 25 mL upon which acetonitrile (50 mL) was added. The solvent mixture was reevaporated to 25 mL, and the procedure was repeated a further two times. The filtrate was filtered through a 0.45-μm Metricel filter (Acrodisc-CR, Gelman Sciences) and reduced to a thin film which was lyophilized with benzene (5 mL); bis-SorbPC was stored in freshly distilled benzene as an amourphous ice (−10 °C) after bubbling with argon for 30 min. Yield: 545 mg (66% based on GPC). TLC showed one spot after development with iodine, R_f = 0.48–0.40 (65:25:4, $CHCl_3/CH_3OH/H_2O$). ^1H NMR d 1.20–1.40 (br s, 20 H, $C\underline{H}_2$), 1.48–1.70 (m, 8 H, $C\underline{H}_2CH_2R$), 1.80–1.88 (d, 6 H, $=CHC\underline{H}_3$), 2.20–2.32 (m, 4 H, $\underline{CH}_2CO_2$), 3.30–3.40 (s, 9 H, $NC\underline{H}_3$), 3.75–3.83 (br s, 2 H, $NC\underline{H}_2CH_2$), 3.88–4.00 (br s, 2 H, $NCH_2C\underline{H}_2$), 4.05–4.12 (t, 4 H, $=CHCO_2C\underline{H}_2$), 4.14–4.42 (br m, 4 H, $POC\underline{H}_2CH$ and $CHC\underline{H}_2O_2C$), 5.14–5.25 (br s, 1 H, $POCH_2C\underline{H}$), 5.72–5.80 (d, 2 H, $O_2CC\underline{H}=$), 6.05–6.24 (m, 4 H, $CH_3C\underline{H}=C\underline{H}$-), 7.16–7.28 (m, 2 H, $C\underline{H}=CHCO_2$). UV: λ_{max} = 258 nm, CH_3OH, ϵ = 47 100.

Methods

Preparation of Liposomes. Unilamellar liposomes as well as oligolamellar liposomes consisting of DOPE or DOPC in a 3:1 molar ratio with bis-SorbPC were prepared by extrusion (Hope et al., 1985; Mayer et al., 1986; Nayar et al., 1989). Bis-SorbPC (8 μmol) from a stock solution was mixed with the appropriate lipid (24 μmol) in a 10-mL flask. Organic solvent was removed on a rotary evaporator leaving a thin lipid film which was further dried under high vacuum for a minimum of 12 h. The lipids were hydrated with the dye marker in buffer to give a concentration of 10 mM, vortexed to a uniform suspension (approximately 2 min) followed by 10 freeze–thaw cycles (−70 → 25 °C). The extruder (Lipex Biomembranes, Inc.) was warmed to 40 °C and the extrusion performed 10 times through two 0.1- or 0.6-μm pore size polycarbonate membranes (Nuclepore Corp.); N_2 pressure was adjusted from 200 psi for 0.1-μm to 50 psi for 0.6-μm pore size membranes.

In some instances liposomes, from DOPE, TPE, or DOPC in either a 3:1 or a 2:1 molar ratio with bis-SorbPC, were prepared by brief sonication with a cup-horn sonicator (Heat Systems-Ultrasonic, Inc.). Lipid mixture suspensions (8–10 mM) were prepared in a similar fashion as above. Sonication was performed for 2 min at 20% output power at 25 °C. Samples were allowed to anneal for 20 min and then extruded through 0.4-μm pore size polycarbonate membranes (Nucleopore). Liposomes were also prepared by the reverse-phase evaporation (REV) method (Szoka & Papahjopoulos, 1978). The total lipids (24 μmol) were dissolved in 3 mL of diethyl ether and combined with 1 mL of the desired buffer and water-soluble dye. This mixture was vortexed and bath sonicated at 5 °C to form an emulsion, which was then reduced in volume by removal of most of the ether on a rotary evaporator. An additional 2 mL of buffer and dye was added, and rotavaporation of the sample was continued to remove the residual ether. The resulting liposome suspension was extruded through 0.4-μm pore size membranes.

Liposomes prepared by each of the above methods were separated from unencapsulated material on either a Bio-Gel P-6DG (Bio-Rad) or a medium Sephacryl S-300 (Pharmacia) column using the appropriate elution buffer. The pooled liposome fractions were diluted with buffer to an optical density of 2.0–2.4 at 258 nm for use in photolysis.

Light Scattering. Liposome distribution was measured using dynamic laser light scattering (Brookhaven BI-8000AT correlator with a 5-mW He–Ne laser light source; Brookhaven Instruments Corp.). Samples were examined at angles of 60°, 90°, and 120° with various fitting methods (e.g., nonnegative least squares, exponential sampling, and CONTIN) used to extract the set of exponential functions which made up the autocorrelation functions.

Liposome Photolysis. Liposome samples (2 mL) having an optical density between 2.0 and 2.4 at 258 nm were bubbled with argon for 2 min and placed 4 cm away from a low-pressure mercury vapor lamp (incident flux of ~5 × 10^{14} photons/s). Photopolymerization was carried out continuously for each new sample; photolysis times ranged from 0 to 30 min. Extent of monomer loss was calculated by a decrease in the absorbance of the sorbyl moiety at 258 nm: $\{[(A_0 - A_t)/(A_0 - A_\infty)] \times 100\}\%$, where A_∞ equals the absorbance after 30 min of photolysis (99% loss of monomer). Ultraviolet spectra were determined on a HP 8452 diode array spectrophotometer (Hewlett Packard) and were run in either buffer or methanol. A Corning CS-9-54 filter (>230 nm) was used to prevent bleaching of the water-soluble dyes.

Fluorescence Assays. Fluorescence spectra were determined on a Spex Fluorolog 2 spectrophotometer with a Datamate data aquisition system (Spex Industries, Inc.). Recorded fluorescence intensities gave a stable value over at least 3 min.

Calcein permeability of liposomes of different size and lipid composition was measured with liposomes containing a self-quenched 75 mM calcein solution (pH 7.4) as the encapsulated fluorophore (Allens & Cleland, 1980). Liposomes prepared by either extrusion or sonication were separated from exterior dye as above using 150 mM NaCl, 2 mM imidazole, and 2 mM TES (pH 7.4) elution buffer. Liposome leakage upon photolysis was registered as an increase in fluorescence as the self-quenched calcein is diluted in the external volume. The leakage scale was calibrated with the fluorescence of a standard liposome solution (before photolysis) as 0% leakage. The fluorescence intensity observed after the liposomes were lysed with 5% Triton X-100 (50 μL) was taken as 100% dye leakage. Excitation was at 490 nm, and the emission was monitored at 550 nm (excitation slit 1.25 cm, emission slit 2.5 cm). Percent leakage of calcein was calculated by $\{[(I_t - I_o)/(I_{Triton} - I_o)] \times 100\}\%$.

ANTS/DPX leakage of liposomes was investigated using the procedure of Ellens et al. (1984). Liposomes were prepared in 12.5 mM ANTS, 12.5 mM NaCl, 25 mM DPX, and 20 mM Tris-HCl at pH 7.5 by sonication. Elution buffer for size exclusion chromatography was 100 mM NaCl, 20 mM Tris HCl, and 0.1 mM EDTA, pH 7.5. Liposomes were photopolymerized as described above. The fluorescence level for 0% leakage was set before photopolymerization. Complete leakage was determined after disrupting the photolyzed liposomes with 5% Triton X-100. The excitation wavelength was 360 nm with the emission maximum occurring at 530 nm. It

should be noted that ANTS is sensitive to exposure to UV light below 220 nm; therefore, the polymerization was performed with a 230-nm filter.

^{31}P NMR Spectroscopy of Extruded Liposomes. Liposomes were buffered with 10 mM HEPES/150 mM NaCl at pH 7.4 (containing 10% D_2O) to a concentration of 24 mM and extruded as above through either 0.1- or 0.6-μm pore size polycarbonate membranes. A capillary external reference containing triphenylphosphine oxide was used to calibrate individual samples before and after the addition of a relaxation agent. The phosphorus FT-NMR spectra were obtained on a Bruker AM-250 spectrometer with an Aspect 3000 computer using 10-mm tubes. A total of 7000 scans were collected with a pulse width of 24 μs and relaxation delay of 2 s. Exponential line broadening of 50 Hz was used. Afterward, the liposome sample was treated with a $MnCl_2$ solution to raise the external concentration to 2 mM Mn^{2+}, and the experiment was repeated as above.

^{31}P NMR Spectroscopy of Extended Bilayers. Samples of DOPE/SorbPC (3:1) were prepared by transferring the pure lipids in $CHCl_3$ to an 8-mm glass tube, where they were mixed, dried, and then redissolved in benzene and lyophilized to remove any residual solvent and water. The lipid mixture was hydrated with buffer (2 mM TES, 2 mM imidazole, and 150 mM NaCl, pH 7.4) to a concentration of about 100 mg/mL. In order to ensure that no small liposomes were present in the sample, it was freeze–thawed at least 10 times in 2-propanol/dry ice and allowed to warm from the last freeze at 4 °C for 20–30 min. The 33% polymerized sample was prepared by exposure of the extended bilayers in a 1-mm quartz cuvette to light from a low-pressure mercury lamp (15 mm from the sample) for 1.25 h. The temperature was maintained at 30.0 ± 0.2 °C during the photolysis. The loss of the monomer was determined spectrophotometrically by the decrease in the sorbate absorption. The ^{31}P NMR experiments were performed with 20–30 mg of lipid sample sealed in an 8-mm glass tube, which was placed in a 10-mm NMR tube containing ethylene glycol. The latter provided good thermal contact between the sample and the probe. The temperature was controlled to ±0.2 °C with the variable temperature unit of the NMR instrument. Constant hydration was maintained by the presence of a reservoir of water in the NMR tube. Proton-decoupled ^{31}P NMR spectra were acquired on a General Electric GN-500 spectrometer operating at 202.5 MHz (11.7 T) using the phase-cycled pulse sequence $(90°-\tau_1-180°-\tau_2-\text{acquisition})_n$. The number of acquisitions, n, ranged from 4500 to 6000, the 90° pulse length was 25 μs, the period τ_1 was 13 μs, the time before acquisition τ_2 was 10 μs, and the recycle time between sequences was 2 s. A line broadening of 80 Hz was used by applying an exponential multiplication function to the free induction decay before Fourier transformation.

Electron Microscopy. Liposome samples were prepared by extrusion as described above (lipid concentration 10 mM). An aqueous film was formed by placing a 10-μL drop on 270 mesh copper grids. After placement of the droplet, it was blotted for approximately 5 s to remove excess suspension. Grids were then immediately plunged into liquid propane to vitrify the water suspension (Talmon et al., 1990). The vitrified samples were transferred under liquid nitrogen to a Gatan cryoholder (model 262) and examined in a Philips model EM420. The samples were maintained at a temperature of −165 °C while in the TEM. Images were recorded photographically.

Differential Scanning Calorimetry. Samples were dried in a fashion similar to those used in liposome preparation. The lipid film was hydrated to a concentration of 1.0 mg/mL with 10 mM Na_2HPO_4/150 mM NaCl at pH 7.4 followed by vigorously vortexing the sample at 40 °C for 3 min until uniformity was observed. The suspension was subjected to 10 freeze–thaw cycles. Thermograms were obtained using a Microcal MC-2 calorimeter at a scan rate between 10 and 15 °C/h. Samples were scanned a minimum of three times.

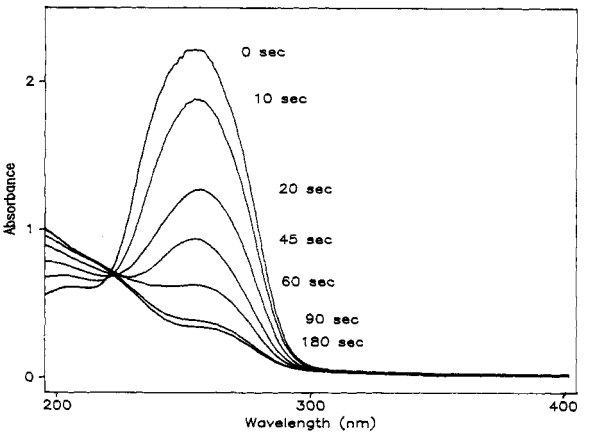

FIGURE 1: Photolysis of SorbPC liposomes in water which were prepared by extrusion through 0.1-μm pore size polycarbonate membranes. Each spectrum was obtained from samples that were flushed with argon, followed by continuous exposure to light from a low-pressure Hg lamp.

RESULTS

Polymerization of SorbPC Membranes

Liposomes of bis-SorbPC (SorbPC, **1**) in aqueous buffer show a λ_{max} at 258 nm at 25 °C and are readily polymerized by irradiation with 254-nm light. Isotropic solutions of **1** in organic solvents show a similar absorption maximum, which indicates that the two sorbyl chromophores per molecule do not strongly interact in the bilayer interior. Only when liposomes of **1** are cooled below their main transition temperature, T_m, do they show a hypsochromic shift due to chromophore aggregation. Liposomes prepared from the longer chain bis-SorbPC(C_{12}) (dodecyl vs decyl spacer group) show a hypsochromic shift to 242 nm with a diminished extinction coefficient at room temperature (Tyminski et al., 1987). Since the bilayers of bis-SorbPC(C_{12}) exist in the gel state at room temperature (T_m = 33 °C for extended bilayers), the all-trans extended conformation will place the chromophores in close apposition favoring aggregation. Warming the liposomes to $>T_m$ caused the absorption maximum to shift to 257 nm.

The principle absorption band of **1** is diminished during the irradiation of liposomes with UV light (Figure 1). This loss of monomer absorption coincides with progressive decrease in sample mobility on thin layer chromatography. The absorbance decrease at 258 nm is accompanied by an increase at approximately 195 nm. An isosbestic region at 222 nm suggests that the photolysis yields primarily one photoproduct. The presence of an isosbestic region rather than a point may be due to small changes in the liposome suspension turbidity during photolysis or a result of the formation of major and minor photopolymer products. Three distinct products are possible via either 1,2-, 1,4-, or 3,4-polymerization. The absorption spectrum is consistant with the formation of a nonconjugated carbon–carbon double bond, which rules out the formation of acrylic moieties via 3,4-polymerization. Since the photopolymerization of **1** yields a cross-linked polymer, which is due in all likelihood to the unequal depth of penetration of the reactive α and β chains (Lopez et al., 1982;

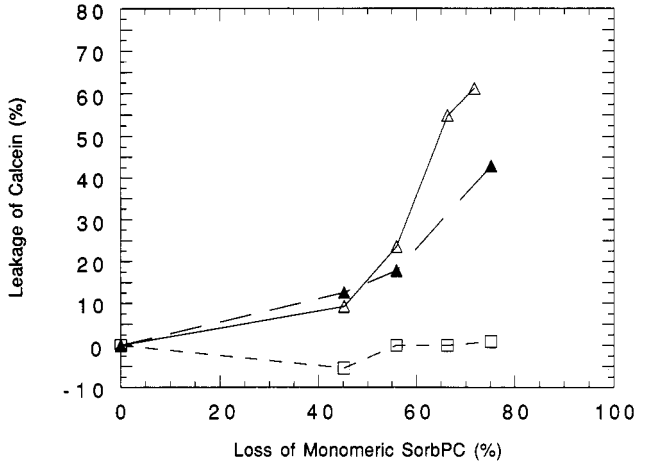

FIGURE 2: Leakage of calcein at 25 °C from liposomes vs the loss of monomeric SorbPC during photopolymerization. The percent leakage was calculated from the increase in calcein fluorescence intensity. Liposomes were prepared by reverse-phase evaporation in a 2:1 molar ratio of DOPE/SorbPC (▲), TPE/SorbPC (△), and DOPC/SorbPC (□) as described under Materials and Methods.

Tyminski et al., 1987), it is difficult to further characterize the polymer structure of **1**. In order to learn more about the polymer structure and size, a sample of the mono-SorbPC (**2**),

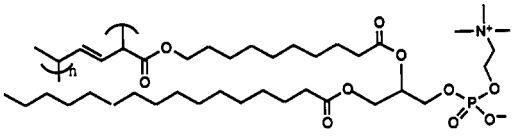

1,4-Polymer from *mono*-SorbPC (2)

which forms linear polymer chains, was photopolymerized in bilayers. The resulting sample was lyophilized, and the polymer was dissolved in chloroform-d_1. ^{1}H NMR of the lipid polymer shows that all of the proton resonances due to the sorbyl moiety have disappeared. The loss of the conjugated terminal methyl signal (1.85 ppm, doublet) and vinyl proton adjacent to the carbonyl (5.72–5.80 ppm, doublet) indicate that this polymer product was formed via a 1,4-polymerization. Photopolymerization of a similar amphiphilic diene, docosadienoic acid, in monolayers reportedly proceeds via a 1,4-polymerization (Ringsdorf & Laschewsky, 1988). Preliminary polymer size data obtained by size exclusion chromatography indicates the mono-SorbPC polymers range from 10 to 100 repeat units depending on the intensity of the light exposure. The relatively short size of the polymers is consistent with the nature of photoactivated polymerizations in contrast to radical chain polymerizations (Guillet, 1985).

Effect of Photopolymerization on Liposome Permeability

Liposomes composed of DOPE/**1**, TPE/**1**, or DOPC/**1** in either a 2:1 or 3:1 molar ratio were prepared by a variety of methods, including mild sonication of hydrated bilayers, reverse-phase evaporation, and extrusion, and were then examined for their ability to encapsulate water-soluble fluorescent markers both before and during photopolymerization of the SorbPC. Most of the experiments were performed with the established calcein assay, whereas the ANTS/DPX leakage assay was used occasionally to test whether the observations were independent of the assay.

(A) *Effect of Liposome Composition.* Figure 2 illustrates a typical calcein permeability experiment. In the examples shown, the liposomes were prepared by reverse-phase evaporation (REV) in the presence of 75 mM calcein buffer and separated from the exterior dye by size exclusion chromatography. Each data point was obtained with a fresh liposome sample of the same original OD at 258 nm and exposed continuously for the indicated time. This procedure is necessary because the size of the lipid polymer chains are controlled by the time and intensity of light exposure. Interruption of light exposure terminates polymer chain growth and reexposure initiates growth at new sites, thereby resulting in lower molecular weight polymers. Each liposome sample was exposed through a 230-nm filter to minimize the light-induced bleaching of the calcein dye. An insignificant amount of calcein was bleached over a 20-min exposure through the filter. As seen in Figure 2, a significant increase in calcein fluorescence is found after a 40–50% loss of monomeric **1** for the PE/**1** liposomes. The increased permeability was clearly detectable after a 1–2-min exposure, and the emission spectra were determined 30 s after the exposure. The fluorescence intensity was constant during the measurement; thus the calcein leakage was complete within 30 s of terminating the polymerization.

Table I: Effect of Liposome Composition and Method of Preparation on the Photoinduced Loss of Calcein from DOPE/SorbPC and DOPC/SorbPC Liposomes at 25 °C

no.	liposome composition and method	% loss of monomeric SorbPC	% calcein leakage
	DOPE/SorbPC (2:1)		
1	REV[a]	56	23
		66	55
2	REV[a]	56	31
		75	50
	DOPC/SorbPC (2:1)		
3	REV[a]	66	0
	DOPE/SorbPC (3:1)		
4	mild sonication	67	18
5	extrusion, 0.6 μm	50	21
		69	27
6	extrusion, 0.6 μm	71	29
7	extrusion, 0.1 μm	50	0
		84	0
	DOPC/SorbPC (3:1)		
8	mild sonication	65	1
9	extrusion, 0.6 μm	56	0
10	extrusion, 0.1 μm	50	1

[a] The liposomes were prepared by reverse-phase evaporation.

Table I summarizes the calculated calcein leakage for illustrative examples of DOPE/**1** and DOPC/**1** at 25 °C. The leakage is reported for selected fractions of lipid photopolymerization derived from experiments such as that shown in Figure 2. The experimental data show that progressive photolysis of the DOPE/**1** liposomes increases the membrane permeability to encapsulated self-quenched calcein. In contrast, irradiation of the DOPC/**1** control membranes did not increase the membrane permeability even after greater than 80% polymerization.

The experiments shown in Figure 2 were performed with relatively large REV liposomes in order to enhance the fraction of the calcein encapsulated in the liposomes. Samples prepared by mild sonication of hydrated bilayers also showed significant photoinduced leakage if the liposomes were composed of DOPE/**1** or TPE/**1**, but not DOPC/**1** (Frankel et al., 1989). Extensive sonication, which is usually associated with the progressive conversion of lipid samples to small unilamellar liposomes, tended to decrease the encapsulation efficiency of the liposomes as expected. Suprisingly, prolonged sonication also tended to decrease the percent of the entrapped calcein that could be released by photolysis of the PE/**1** liposomes.

The photoinduced leakage of PE/**1** membranes was confirmed with a second assay. Both a fluorescent dye, 8-

Table II: Liposome Size of DOPC/SorbPC and DOPE/SorbPC (3:1) Liposomes as a Function of Preparation

liposome preparation	diameter[a] (nm)	mole fraction	
		inner lipid[b]	outer lipid[b]
extrusion, 0.1 μm	125 ± 15	0.47 ± 0.02	0.53 ± 0.02
extrusion, 0.6 μm	275 ± 65	0.84 ± 0.06	0.16 ± 0.01
sonication[c]	320 ± 70	nd	nd

[a] Determined by dynamic laser light scattering. [b] Determined for the DOPC/SorbPC liposomes by ^{31}P NMR spectroscopy with $MnCl_2$. [c] Sonicated in polycarbonate tubes for 2 min at 20% power; nd, not determined.

aminonaphthalene-1,3,6-trisulfonate sodium salt (ANTS), and its quencher, *p*-xylylene-bis-pyridinium bromide (DPX), were encapsulated in the liposomes (see Methods). DPX quenches the fluorescence of ANTS by classical Förster energy transfer rather than a complex formation. Any process that causes the dye and quencher to leak from the liposomes will result in their dilution with a consequent immediate decrease in the efficiency of DPX quenching of the ANTS fluorescence (Ellens et al., 1984). The photoinduced loss of monomeric **1** results in an increased ANTS fluorescence for both the DOPE/**1** and TPE/**1** membranes. The observed fluorescence increase occurred after 30–40% polymerization of the bis-SorbPC. In contrast, the fluorescence intensity does not change even after 80% polymerization of the DOPC/**1** liposomes.

(B) *Effect of Liposome Size and Lamellarity.* In order to characterize the nature of the lipid structure responsible for the destabilization of the photolyzed PE/SorbPC liposomes, a parallel investigation of the ^{31}P NMR spectra of extended bilayers of DOPE/SorbPC was undertaken (see ^{31}P NMR below). The progressive appearance of an isotropic NMR signal at the expense of the lamellar signal suggested that a lipid structure with isotropic symmetry was associated with the photoinduced leakiness of the DOPE/SorbPC liposomes. The ^{31}P NMR studies were performed with extended bilayers, where interaction between bilayers is convenient. Bilayer contact of PE lamellae leading to the formation of nonlamellar structures has previously been described as a prerequisite for liposome destabilization (Ellens et al., 1984, 1985, 1986; Allen et al., 1990). The theoretical analysis of Siegel (1984, 1986) indicates that nonlamellar structures form much more rapidly from apposed exterior monolayers than from within one lamella. On the other hand, the photoinduced permeability studies illustrated in Figure 2 and Table I were performed with liposomes, where bilayer contact can take two forms. Intraliposomal bilayer contact in a liposome could occur between lamellae, if the liposome has more than one bilayer (oligo- or multilamellar). Interliposomal bilayer contact could occur between the exterior monolayers if two or more liposomes associate.

In order to test whether bilayer contact is necessary for the photoinduced destabilization of DOPE/**1** membranes, liposomes of different sizes and lamellarity (unilamellar versus oligolamellar) were prepared by extrusion (Hope et al., 1985). Table II describes the size of liposomes prepared by extrusion and sonication. Liposomes (DOPE/**1** and DOPC/**1**) prepared by extrusion through either 100- or 600-nm diameter pore size Nuclepore filters were found by dynamic light scattering to have an apparent diameter, respectively, of either 125 nm with a narrow polydispersity or 275 nm with a broader polydispersity. Samples of both sizes of the DOPC/**1** liposomes were examined for the accessibility of the lipid phosphate groups to an externally added relaxation reagent, Mn^{2+} (Michaelson et al., 1973; Berden et al., 1975). These data indicate that the 125-nm diameter liposomes are unilamellar, because

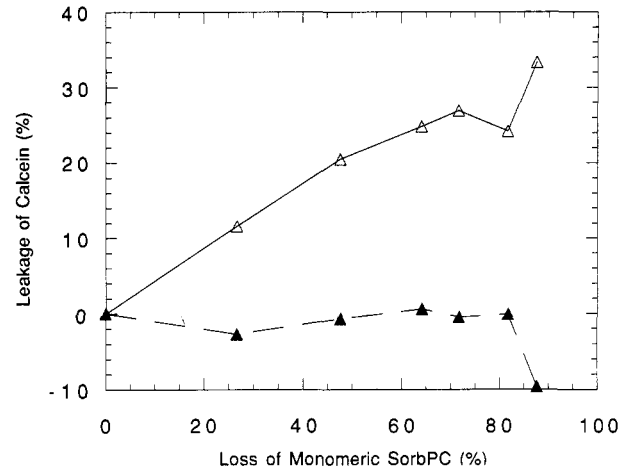

FIGURE 3: Calcein leakage at 25 °C of DOPE/SorbPC (3:1) liposomes prepared by extrusion through 0.1-μm (▲) and 0.6 μm (△) pore size polycarbonate membranes versus the loss of monomeric SorbPC.

slightly more than half of the lipid phosphate group signal was relaxed by the addition of the Mn^{2+}. In contrast, the 275-nm liposomes have only 16% of the phosphates available for interaction with the externally added Mn^{2+}, which indicates the presence (on average) of several lamellae per liposome. For convenience, we will refer to these two preparations as unilamellar (estimated diameter 125 nm) and oligolamellar (estimated diameter 275 nm). Previous reports on extruded liposomes of other lipid compositions concluded that 100-nm diameter liposomes are generally unilamellar, whereas liposomes greater than 200 nm in diameter are progressively more oligo- or multilamellar (Ellens et al., 1989). Both the 125- and 275-nm diameter liposomes of DOPE/**1** were examined by cryotransmission electron microscopy. The images of 125-nm liposomes indicate they were predominantly unilamellar, whereas the images of larger liposomes showed a relatively high proportion (40–50%) of oligolamellar structures in the samples examined.

Figure 3 illustrates the effect of liposome size on the photoinduced leakage of calcein from DOPE/**1** (3:1) liposomes. Photoinduced release was observed only with the oligolamellar liposomes, but not with the unilamellar DOPE/**1** liposomes. This pair of experiments was confirmed in each of three trials. Neither unilamellar nor oligolamellar DOPC/**1** liposomes were destabilized by photopolymerization of the SorbPC (Table I, experiments 7, 9, and 10).

The necessity of bilayer contact for liposome destabilization was previously reported for PE/CHEMS unilamellar liposomes. The H^+-induced leakage of these liposomes required liposome–liposome bilayer contact for systems either below or above their T_H (Ellens et al., 1984). A similar effect was seen in the H^+ and Ca^{2+} destabilization of PE vesicles at their T_H (Ellens et al., 1986a). However, an additional first-order kinetic process which led to leakage was observed. This first-order process is due to the collapse of oligolamellar liposomes following bilayer contact within the liposome. In a similar manner, the photoinduced destabilization of DOPE/**1** liposomes could occur either via inter- and/or intraliposomal bilayer contact:

$$V_1 + V_1 \underset{}{\overset{\text{aggregation}}{\rightleftharpoons}} V_2 \rightarrow N_2 \xrightarrow{\text{leakage}} \quad (1)$$

$$V_1 \rightarrow N_1 \xrightarrow{\text{leakage}} \quad (2)$$

In the above equations, N_1 and N_2 represent liposomes with nonlamellar phases. Equation 1 indicates a destabilization process which occurs through the aggregation of at least two

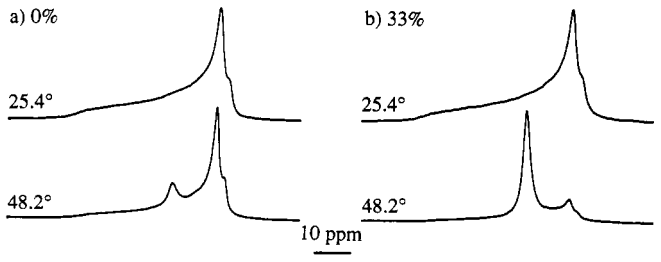

FIGURE 4: ^{31}P NMR spectra of extended bilayers of DOPE/SorbPC (3:1) at 25.4 and 48.2 °C. The spectra on the left (a) are from an unpolymerized sample, and the spectra on the right (b) are for a sample where the loss of monomeric SorbPC is 33%. The sharp edges of the L_α phase powder patterns (the 90° orientation of the bilayer normal with respect to the magnetic field) are resolved for the PE and PC, with the smaller outermost signal corresponding to the PC. Note that the 90° edges of the L_α phase powder patterns are enhanced in intensity, indicating that the 11.7 T field was strong enough to cause some of the bilayers to orient in the magnetic field.

liposomes (V_2) with the formation of a nonlamellar phase involving both liposomes. Equation 2 represents destabilization due to intraliposomal interaction between apposing lamellae. Equation 1 is the sole mechanism of leakage for unilamellar liposomes. Oligolamellar liposomes may leak via the processes represented by eqs 1 and 2 and will depend upon the concentration of the sample. At high liposome concentration, interliposomal contact and eq 1 will predominate; in more dilute solutions, eq 2 becomes the mechanism of choice since interliposomal interactions are reduced.

In distinguishing between inter- or intraliposomal bilayer contact in the photoinduced destabilization of DOPE/SorbPC liposomes, the same lipid concentration was used in both unilamellar and oligolamellar liposomes by adjusting the optical density of the sample on the basis of the sorbyl moiety (λ_{max} = 258 nm) to 2.3 OD. Since the larger vesicles consist of several lamellae, the liposome concentration was greater for the unilamellar then the oligolamellar sample, e.g., 275-nm diameter liposomes with five lamellae with a 20-nm spacing between lamellae have 18 times more lipid/liposome than a 125-nm unilamellar liposome. Destabilization of unilamellar liposomes can only occur via interliposomal contact of lamellae during photopolymerization (eq 1). The inability of these unilamellar liposomes to undergo leakage suggests that the liposome concentration is too dilute for liposome–liposome interactions. The observed leakage from the oligolamellar liposomes of the same lipid concentration must occur between the lamellae within the liposome (eq 2), because the probability of liposome–liposome interaction is at least an order of magnitude less than that of unilamellar liposomes.

^{31}P NMR Spectroscopy of DOPE/SorbPC Extended Bilayers. The ^{31}P NMR spectra of extended bilayers of both unpolymerized DOPE/**1** (3:1) and partially (33%) photopolymerized DOPE/**1** (3:1) are shown in Figure 4. These samples were each examined at several temperatures in order to outline the phase behavior of the lipid mixtures. Here we emphasize the behavior at 25.4 and 48.2 °C to point up the differences in behavior of the sample before and after partial polymerization of the SorbPC in the bilayers. A full paper which describes the complete NMR study and complementary X-ray diffraction experiments on these extended bilayers is in preparation.[2] Both samples at 25.4 °C display lamellar powder patterns. However, as the samples were heated, they each showed the progressive formation of an isotropic signal in competition with the lamellar pattern. The mixtures were heated slowly at a rate of 2.5–10 °C per hour, in increments of 2.5 or 5 °C. As seen in Figure 4, the isotropic signal comes to dominate the NMR spectrum of the polymerized DOPE/**1** bilayers by 48.2 °C. Analysis of the relative distribution of lipids between the lamellar and isotropic signals reveals that at 48.2 °C approximately 56% of the lipids contribute to the isotropic signal in the polymerized DOPE/**1**, whereas only 8% of the lipids do the same in the unpolymerized bilayers. Continued heating of each sample to above 60 °C completely converts the NMR spectrum into an isotropic signal, with no lamellar or inverted hexagonal contributions. X-ray diffraction studies on these samples indicate that the extended bilayers of DOPE/**1** could be converted into an inverted cubic phase (Barry et al., 1991; Osterberg et al., 1991). After the NMR spectra were entirely isotropic, they did not change as the samples were cooled to 25 °C. Only with multiple freeze–thaw cycles did the isotropic signal disappear to give the original 25.4 °C spectrum.

Discussion

Both Gaub et al. (1984) and Tyminski et al. (1985, 1987) reported that the photopolymerization of lipid bilayers composed of a polymerizable dienoyl lipid and a nonpolymerizable PC proceeds via phase separation to yield a bilayer of polymerized and nonpolymerized domains. Our studies with the photoactivated polymerization of the analogous sorbyl PC's show they form domains of cross-linked poly-**1**. The polymerization of phospholipid/SorbPC bilayers effectively initiates a change in monomer composition of the bilayer and the lateral distribution of the lipids. The experimental data reported here indicate that if photoinduced phase separation is accompanied by both (1) bilayer contact between apposing lamellae and (2) a lipid composition that includes polymorphic lipids, then the liposomes will be destabilized. In principle, only phase separation might be required for the permeability increase if leakage occurred between the domains of poly-**1** and nonpolymerized lamellar lipids. However, the observed membrane stability of the DOPC/**1** liposomes makes this explanation unlikely. Photoinduced phase separation occurs in PC/poly-**1** membranes, and the domains of PC lamellar phase and poly-**1** coexist without any apparent enhancement of membrane permeability. Thus phase separation alone is insufficient to cause an increase in membrane permeability.

Photoinduced phase separation in membranes of DOPE/SorbPC creates enriched domains of DOPE. Homogeneous bilayers of PE/PC are repelled from neighboring bilayers by strong hydration forces (Parsegian et al., 1979; Rand, 1981). Processes which promote phase separation and cause the enrichment of domains of the less strongly hydrated PE will decrease the repulsive forces in these regions and allow the close approach of some areas of the bilayers. Contact between apposing lamellae enriched in PE in oligolamellar liposomes can lead to the formation of inverted micellar intermediates (IMI), which begins at temperatures below the nonlamellar phase transition. Polymerization lowers the temperature of the lamellar to nonlamellar phase transition (Figure 4);[2] therefore, the number of intermediate structures increase at a given temperature with the formation of polymeric and nonpolymeric domains. A similar effect has been observed in a series of model membranes of DOPE/DOPC where decreased DOPC content leads to a lowering of T_H (Ellens et al., 1987). At the T_H, IMI assemble into the H_{II} phase by coalescing with other IMI's that form between the same two apposed bilayers. The leakage of water-soluble markers could occur due to the conversion of regions of the apposed liposomal

[2] J. A. Barry, H. Lamparski, F. Osterberg, J. Cerne, E. Shyamsunder, M. F. Brown, and D. F. O'Brien (manuscript in preparation).

bilayers into H_{II} structures. However, the ^{31}P NMR spectra of extended bilayers of these lipids (Figure 4) shows that the H_{II} phase is not formed under these conditions, but rather an isotropic symmetric structure grows in competition with the bilayer structure.[2] It is proposed that IMI can form interlamellar attachments (ILA) in competition with the H_{II} phase (Siegel, 1986a,b). An ILA is an hourglass-shaped bilayer attachment between two original lamellae that effectively fuses the original lamellae. ILA's exhibit an isotropic ^{31}P NMR resonance since lipid molecules diffusing along the surfaces of the ILA experience all orientations of their head group with respect to the bilayer normal. Under appropriate circumstances ILA's can proceed to form long-lived arrays which take on the characteristics of the inverted cubic phase.

Photopolymerization of DOPE/SorbPC liposomes could result in an increased prevalence of the IMI → ILA path because of the change in monomeric lipid composition as the polymerization proceeds. Gruner et al. (1988) point out that lipids with intermediate values of the spontaneous radius of curvature R_0 (Kirk et al., 1984; Gruner, 1985) show nonequilibrium phase behavior with the appearance of isotropic as well as H_{II} structures. The DOPE/SorbPC system is originally lamellar until the polymerization of the SorbPC decreases the average R_0 of the remaining monomeric lipids in the DOPE/SorbPC system to the point where the formation of nonequilibrium isotropic structures is favored. Figure 5, which is adapted from Siegel's model (1987) for liposome–liposome fusion, schematically illustrates the light-induced phase separation of poly-**1** and DOPE, which allows the interaction and formation of intermediate lipid structures between bilayers, with the eventual development of an ILA. In this case, we propose that the ILA(s) is between the lamellae of an oligolamellar liposome and provides an aqueous pathway for the leakage of water-soluble encapsulated reagents. Note that Figure 5 shows participation of only the DOPE in the formation of IMI's and ILA's, whereas some of the unpolymerized SorbPC may also be involved in the ILA's. It was found[2] that both DOPE and monomeric SorbPC contribute to the isotropic NMR signals in extended bilayers.

The model is helpful in understanding the apparent digital nature of the release of calcein. It predicts that only photolyzed oligolamellar liposomes in the sample will become leaky and that all the calcein in each of these liposomes will be released rapidly after the formation of the ILA. A threshold for release from some liposomes is achieved when 30–50% of the monomer has reacted. This represents the minimum conditions for the successful perturbation of these compositions of liposomes. Further photopolymerization releases more calcein, which we interpet to mean that liposomes with multiple lamellae require several ILA's in order to release the calcein originally sequestered in the aqueous spaces between all the lamellae. The final proportion of unreleased calcein is probably entrapped in the fraction of unilamellar liposomes that are present in all samples. In addition, we have shown experimentally that all the calcein released from a given photolyzed sample is detectable within 30 s; therefore, the calcein is not slowly leaking out of the liposomes. The rate of release is probably much faster than the time scale of our current experimental protocol. Additional experiments can be envisioned to use this photoactivated chemistry to time resolve the formation of an ILA-mediated permeability pathway.

The formation of ILA's are predicted to mediate the fusion of two liposomes with one another or precede the formation of extensive inverted cubic structures from extended bilayers. In order to further test the relevance of this model to the behavior of photopolymerized PE/SorbPC membranes, we are currently pursuing two studies, which will be described in detail in future papers. First, at higher liposome concentrations than those used in this study, the photopolymerization of PE/SorbPC can initiate liposome–liposome fusion with the mixing of aqueous contents.[3] Second, at high lipid concentration such as that used in the NMR experiments, we would expect the formation of high concentrations of ILA's that proceed to an inverted cubic phase. Bragg diffraction data taken on the DOPE/SorbPC (3:1) membranes show peaks which are indexed to a cubic lattice consistent with the *Pn*3*m* of *Pn*3 space groups (Osterberg et al., 1991). The experiments were performed in the same temperature range where the ^{31}P NMR spectra show a single isotropic peak.

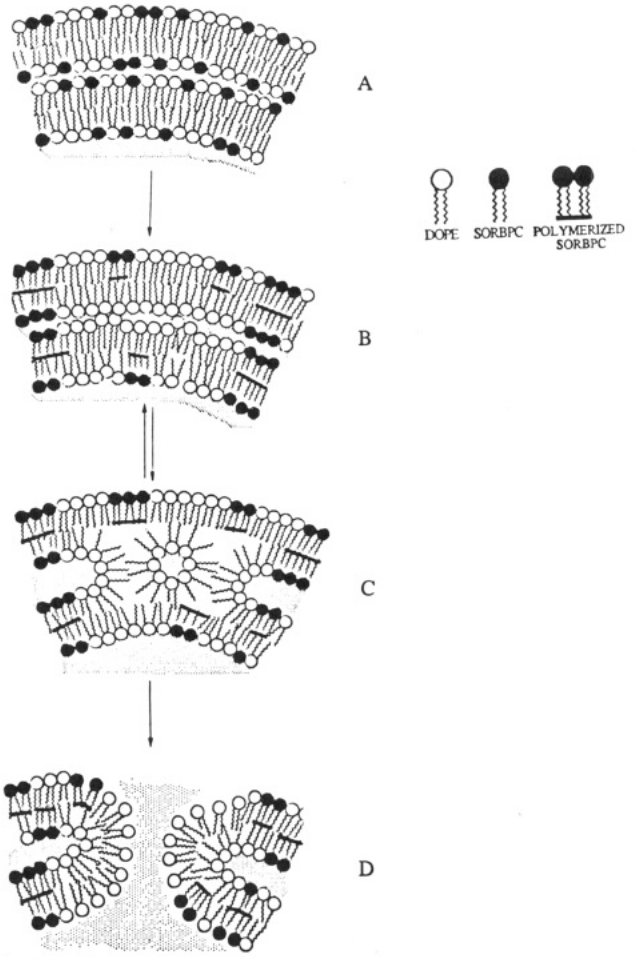

FIGURE 5: Model for intraliposomal destabilization of oligolamellar liposomes. (a) Schematic cross section of two lamellae in a liposome. (b) Photopolymerization of the SorbPC in each lamellae induces separation of lipids into monomeric and polymeric domains, which allows bilayer contact between the enriched domains of PE. (c) Bilayer contact leads to IMI formation. (d) Interlamellar attachment (ILA) between lamellae, which provides a liposomal aqueous channel.

Seddon (1990) noted that it is very difficult to prove that nonlamellar structures play a role in specific dynamic membrane processes, because these processes need only occur in localized regions of the bilayer (here a liposome) for very short times at the temperature of the experiment. This is especially true in comparing our experiments performed with liposomes (photoinduced leakage) and with extended bilayers (^{31}P NMR). The formation of only a very few ILA's per liposome are necessary to account for the observed leakage of aqueous markers from the liposome interior. Approximately 10^3 lipids

[3] U. Liman, D. A. Frankel, D. F. O'Brien (unpublished observations).

may be involved in a single ILA, and there are at least 10^6 lipids in a 275-nm oligolamellar liposome; therefore, only 0.1 mol % of the lipids need to participate in the formation of the destabilizing structures in liposomes. A just detectable isotropic signal observed in the NMR spectrum of extended bilayers of 33% photopolymerized DOPE/SorbPC (3:1) at 34 °C corresponds to 1 or 2 mol % of the lipids.[2] NMR is not sensitive enough to detect the participation of 0.1 mol % of the molecules in an ILA.

We have proposed here that the leakage of aqueous contents in oligolamellar liposomes could occur via a fusion of the lamellae within a single liposome. Such structures are possible in other liposome fusion protocols but are not likely if the liposome destabilization is initiated by the addition of chemical agents, e.g., Ca^{2+}, which do not penetrate the exterior bilayer of the liposome. In those cases, membrane perturbation occurs at the exterior lipid leaflet of the liposome. In contrast, the ability of light to penetrate the liposome results in the initiation of lipid polymerization and formation of enriched PE domains in any of the lamellae of the oligolamellar liposomes. Therefore light can perturb the liposome by the formation of destabilizing intermediates between the lamellae of a single oligolamellar liposome. Finally, it should be noted that the well-known methods of controlling the spatial and temporal delivery of light endow this new technique with a potentially valuable capability to regulate the release of chemical and biological reagents.

Registry No. SorbPC, 124154-20-7; DOPC, 4235-95-4; DOPE, 4004-05-1; 10-(2',4'-hexadienoyloxy)decan-1-ol, 137794-51-5; 2,4-hexadienoic acid, 110-44-1; 10-(2',4'-hexadienoyloxy)decanoic acid, 137794-52-6.

References

Allen, T. M., & Cleland, L. G. (1980) *Biochim. Biophys. Acta 597*, 418–426.

Allen, T. M., Hong, K., & Papahadjopoulous, D. (1990) *Biochemistry 29*, 2976–2985.

Bader, H., Dorn, K., Hupfer, B., & Ringsdorf, H. (1985) *Adv. Polym. Sci. 64*, 1–62.

Bentz, J., Ellens, H., & Szoka, F. C. (1987) *Biochemistry 26*, 2105–2116.

Berden, J. A., Barker, R. W., & Radda, G. K. (1975) *Biochim. Biophys. Acta 375*, 186–208.

Boni, L. T., & Hui, S. W. (1983) *Biochim. Biophys. Acta 731*, 177–185.

Brown, P. M., & Silvius, J. R. (1989) *Biochem. Biophys. Acta 980*, 181–190.

Connor, J., Yatvin, M., Huang, L. (1984) *Proc. Natl. Acad. Sci. U.S.A. 81*, 1715–1718.

Cullis, P. R., & de Kruijff, B. (1978) *Biochim. Biophys. Acta 513*, 31–42.

Cullis, P. R., & de Kruijff, B. (1979) *Biochim. Biophys. Acta 559*, 399–420.

Cullis, P. R., Hope, M. J., de Kruijff, B., Verkeij, A. J., & Tilcock, C. P. S. (1985) in *Phospholipids and Cellular Regulation* (Kuo, J. F., Ed.) pp 1–59, CRC Press, Boca Raton, FL.

Deamer, D. W., Leonard, R., Tardieu, A., & Branton, D. (1970) *Biochim. Biophys. Acta 219*, 47–60.

Duzgunes, N., Straubinger, R. M., Baldwin, P. A., Friend, D. S., & Paphadjopoulos, D. (1985) *Biochemistry 24*, 3091–3098.

Ellens, H., Bentz, J., & Szoka, F. C. (1984) *Biochemistry 23*, 1532–1538.

Ellens, H., Bentz, J., & Szoka, F. C. (1986a) *Biochemistry 25*, 285–294.

Ellens, H., Bentz, J., & Szoka, F. C. (1986b) *Biochemistry 25*, 4141–4147.

Ellens, H., Siegel, D. P., Alford, D., Yeagle, P. L., Boni, L., Lis, L. J., Quinn, P. J., & Bentz, J. (1989) *Biochemistry 28*, 3692–3703.

Epand, R. M. (1985) *Chem. Phys. Lipids 36*, 387–393.

Epand, R. M., & Bottega, R. (1987) *Biochemistry 26*, 1820–1825.

Frankel, D. A., Lamparski, H., Liman, U., & O'Brien, D. F. (1989) *J. Am. Chem. Soc. 111*, 9262–9263.

Gaub, H., Sackmann, E., Buschl, R., & Ringsdorf, H. (1984) *Biophys. J. 45*, 725–731.

Gruner, S. M. (1985) *Proc. Natl. Acad. Sci. U.S.A. 82*, 3665–3669.

Gruner, S. M. (1987) in *Liposomes: From Biophysics to Therapeutics* (Ostro, M. J., Ed.) pp 1–38, Marcel Dekker, New York.

Gruner, S. M., Tate, M. W., Kirk, G. L., So, P. T. C., Turner, D. C., Keane, D. T., Tilcock, C. P. S., & Cullis, P. R. (1988) *Biochemistry 27*, 2853–2866.

Gulik-Krzywicki, T. (1975) *Biochim. Biophys. Acta 415*, 1–28.

Guillet, J. (1985) *Polymer Photophysics and Photochemistry*, Cambridge University Press, Cambridge.

Haubs, M., & Ringsdorf, H. (1985) *Angew. Chem., Int. Ed. Engl. 24*, 882–883.

Haubs, M., & Ringsdorf, H. (1987) *Nouv. J. Chim. 11*, 151–156.

Hong, K., Baldwin, P. A., Allen, T. M., & Papahadjopoulos, D. (1988) *Biochemistry 27*, 3947–3955.

Hope, M. J., Bally, M. B., Webb, G., & Cullis, P. R. (1985) *Biochim. Biophys. Acta 812*, 55–65.

Hui, S. W. (1988) *Curr. Top. Membr. Transp. 29*, 29–70.

Hui, S. W., Stewart, T. P., Boni, L. T., & Yeagle, P. L. (1981a) *Science 212*, 921–923.

Hui, S. W., Stewart, T. P., Yeagle, P. L., & Albert, A. D. (1981b) *Arch. Biochem. Biophys. 207*, 227–240.

Hui, S. W., Stewart, T. P., & Boni, L. T. (1983) *Chem. Phys. Lipids 33*, 113–126.

Kano, K., Yanaka, Y., Ogawa, T., Shimomura, M., & Kunitake, T. (1981) *Photochem. Photobiol. 34*, 323–329.

Kirk, G. L., Gruner, S. M., & Stein, D. L. (1984) *Biochemistry 23*, 1093–1102.

Leventis, R., Gagne, J., Fuller, N., Rand, R. P., & Silvius, J. R. (1986) *Biochemistry 25*, 6978–6987.

Liman, U., Frankel, D. A., & O'Brien, D. F. (1988) *Biophys. J 53*, 325a.

Lindblom, G., & Rilfors, L. (1989) *Biochim. Biophys. Acta 988*, 221–256.

Lopez, E., O'Brien, D. F., & Whitesides, T. H. (1982) *J. Am. Chem. Soc. 104*, 305–307.

Luzzati, V., & Reiss-Hudson, F. (1962) *J. Cell Biol. 12*, 207–219.

Luzzati, V., & Reiss-Hudson, F. (1966) *Nature 210*, 1351–1352.

Luzzati, V., Gulik-Krzywicki, T., & Tardieu, A. (1968) *Nature 218*, 1031–1034.

Mayer, L. D., Hope, M. J., & Cullis, P. R. (1986) *Biochim. Biophys. Acta 858*, 161–168.

Michaelson, D. M., Horwitz, A. F., & Klein, M. P. (1973) *Biochemistry 12*, 2637–2645.

Nayar, R., Hope, M. J., & Cullis, P. R. (1989) *Biochim. Biophys. Acta 986*, 200–206.

O'Brien, D. F., & Ramaswami, V. (1989) in *Encylopedia of Polymer Science and Engineering*, second ed., Vol. 17, pp 108–135, John Wiley and Sons, New York.

Osterberg, F., Cerne, J., Shyamsunder, E., Gruner, S. M., Lamparski, H., & O'Brien, D. F. (1991) *Biophys. J. 59*, 128a.
Parsegian, V. A., Fuller, N., & Rand, R. P. (1979) *Proc. Natl. Acad. Sci. U.S.A. 76*, 2750-2754.
Pidgeon, C., & Hunt, C. A. (1983) *Photochem. Photobiol. 37*, 491-494.
Pidgeon, C., & Hunt, C. A. (1987) *Methods Enzymol. 149*, 99-111.
Rand, R. P. (1981) *Annu. Rev. Biophys. Bioeng. 10*, 277-314.
Regen, S. L. (1987) in *Liposomes: From Biophysics to Therapeutics* (Ostro, M. J., Ed.) p 73, Marcel Dekker, New York.
Ringsdorf, H., & Laschewsky, A. (1988) *Marcromolecules 21*, 1936-1941.
Ringsdorf, H., Schlarb, B., & Venzmer, J. (1988) *Angew. Chem., Int. Ed. Engl. 27*, 113-158.
Seddon, J. M. (1990) *Biochim. Biophys. Acta 1031*, 1-69.
Shyamsunder, E., Gruner, S. M., Tate, M. W., Turner, D. C., So, P. T. C., & Tilcock, C. P. S. (1988) *Biochemistry 27*, 2332-2336.
Siegel, D. P. (1984) *Biophys. J. 45*, 399-420.
Siegel, D. P. (1986a) *Biophys. J. 49*, 1155-1170.
Siegel, D. P. (1986b) *Biophys. J. 49*, 1171-1183.
Siegel, D. P. (1987) *Chem. Phys. Lipids 42*, 279-301.
Siegel, D. P., Burns, J. L., Chestnut, M. H., & Talmon, Y. (1989a) *Biophys. J. 56*, 161-169.
Siegel, D. P., Banschbach, J., Alford, D., Ellens, H., Lis, L. J., Quinn, P. J., Yeagle, P. L., & Bentz, J. (1989b) *Biochemistry 28*, 3703-3709.
Strolley, J. G., & Vail, W. J. (1977) *Biochim. Biophys. Acta 471*, 372-390.
Szoka, F. C., & Papahadjopoulos, D. (1978) *Proc. Natl. Acad. Sci. U.S.A. 75*, 4194-4198.
Talmon, Y., Burns, J. L., Chestnut, M. H., & Siegel, D. P. (1990) *J. Electron Microsc. Tech. 14*, 6-12.
Tilcock, C. P. S., Bally, M. B., Farren, S. B., & Cullis P. R. (1982) *Biochemistry 21*, 4596-4601.
Tyminski, P. N., Latimer, L. H., & O'Brien, D. F. (1985) *J. Am. Chem. Soc. 107*, 7769-7770.
Tyminski, P. N., Ponticello, I. S., & O'Brien, D. F. (1987) *J. Am. Chem. Soc. 109*, 6541-6542.
Tyminski, P. N., Latimer, L. H., & O'Brien, D. F. (1988) *Biochemistry 27*, 2696-2705.
Van Dijck, P. W. M., de Kruijff, B., Van Deenen, L. L. M., de Grier, J., & Demel, R. A. (1976) *Biochim. Biophys. Acta 455*, 576-587.
Veiro, J. A., Khalifah, R. G., & Rowe, E. (1990) *Biophys. J. 57*, 637-641.
Verkleij, A. J. (1984) *Biochim. Biophys. Acta 779*, 43-66.
Verkleij, A. J., de Maagd, R., Leunissen-Bijvelt, J., & de Kruijff, B. (1982) *Biochim. Biophys. Acta 684*, 255-262.
You, H., & Tirrell, D. A. (1991) *J. Am. Chem. Soc. 113*, 4022-4023.

Investigation of Heme Distortions and Heme–Protein Coupling in the Isolated Subunits of Oxygenated Human Hemoglobin by Resonance Raman Dispersion Spectroscopy

Reinhard Schweitzer-Stenner,* Uwe Dannemann, and Wolfgang Dreybrodt
Institute of Experimental Physics, University of Bremen, 2800 Bremen 33, Germany
Received June 27, 1991; Revised Manuscript Received October 10, 1991

ABSTRACT: To probe the distortions of the heme groups resulting from heme–apoprotein interaction in the isolated subunits of oxygenated human hemoglobin (i.e., α^{SH}-oxyHbA and β^{SH}-oxyHbA), the dispersion of the depolarization ratio of the Raman lines at 1375 cm^{-1} (ν_4) and 1638 cm^{-1} (ν_{10}) was measured at various pHs. The data were analyzed in terms of vibronic coupling parameters which depend on symmetry-classified normal distortions of the heme groups. In the α-chain the ν_{10} mode is not affected by symmetry-lowering distortions. In the β-chain, however, this mode is significantly influenced by asymmetric B_{1g} and B_{2g} distortions. This was interpreted in terms of different interactions between the peripheral substituents and the porphyrin macrocycle in the respective chains. The ν_4 mode of both chains is subject to B_{1g} (B_{2g}) and A_{2g} distortions, which are more pronounced in β^{SH}-oxyHbA. This is most probably due to differences in the repulsive interactions between the proximal imidazole and the pyrrole. While the depolarization ratio of both lines investigated is pH-independent in α^{SH}-oxyHbA, it exhibits a significant pH dependence in β^{SH}-oxyHbA. This parallels the finding that the isolated β-chains exhibit a Bohr effect whereas the α-chains do not. Consequently, the pH dependence of the coupling parameters and the Bohr effect of β^{SH}-oxyHbA could be rationalized in terms of the very same proton binding processes. Moreover, the Raman data correlate with low-temperature kinetic measurements by DeIorio et al. [(1990) *Biophys. J. 59*, 1-13] which reveal that the β^{SH}-Hb exhibits a larger structural heterogenity than α^{SH}-Hb. This indicates that the normal distortions monitored by vibronic coupling matrix elements are provided by different conformational substates of the porphyrin macrocycle.

The thorough understanding of cooperativity of oxygen binding to hemoglobin requires knowledge about the modulation of the tertiary structure of its subunits by their aggregation into functional $\alpha_2\beta_2$ tetramers. Moreover, it is im-

0006-2960/92/0431-694$03.00/0